JPE 16-1-10

http://dx.doi.org/10.6113/JPE.2016.16.1.84
ISSN(Print): 1598-2092 / ISSN(Online): 2093-4718

Loss Analysis and Soft-Switching Behavior of Flyback-Forward High Gain DC/DC Converters with a GaN FET

Yan Li†, Trillion Q. Zheng*, Yajing Zhang*, Meiting Cui*, Yang Han**, and Wei Dou**

†,*School of Electrical Engineering, Beijing Jiaotong University, Beijing, China
**Beijing Corona Science & Technology Co.,Ltd, Beijing, China

Abstract

Compared with Si MOSFETs, the GaN FET has many advantages in a wide band gap, high saturation drift velocity, high critical breakdown field, etc. This paper compares the electrical properties of GaN FETs and Si MOSFETs. The soft-switching condition and power loss analysis in a flyback-forward high gain DC/DC converter with a GaN FET is presented in detail. In addition, a comparison between GaN diodes and Si diodes is made. Finally, a 200W GaN FET based flyback-forward high gain DC/DC converter is established, and experimental results verify that the GaN FET is superior to the Si MOSFET in terms of switching characteristics and efficiency. They also show that the GaN diode is better than the Si diode when it comes to reverse recovery characteristics.

Key words: EPC, Flyback-forward, GaN FET, GaN Schottky diode, High gain, Loss analysis

I. INTRODUCTION

With the ever increasing power demands of modern systems, as well as the desire for reduced size and lower power consumption, high power density and high efficiency are the key drivers for the advancement of power conversion technologies. However, devices based on Si semiconductor materials are approaching the limits of physical performance with respect to lowering power conversion losses, particularly in terms of reducing conduction resistance and switching loss. Wide band-gap semiconductor materials such as silicon carbide (SiC) and gallium nitride (GaN) have many advantages including a wide band gap, high saturation drift velocity, high critical breakdown field, etc. As a result, wide band-gap semiconductor devices are more suitable for high-frequency, high-temperature, high power density and high efficiency applications [1]-[4]. Currently, a series of breakthroughs on SiC devices have been made. However, the research and application of GaN devices is still limited [5]-[8]. EPC, Transphorm, GaN systems and Panasonic Inc. have GaN devices. These GaN devices can be categorized into two types defined by their physical structure: single enhancement mode and cascade mode. In these devices, a low voltage Si MOSFET is in series to drive a depletion mode GaN HEMT. Compared to cascade mode devices, these enhanced mode devices usually have a lower on-resistance and smaller size. As a result, they are more attractive for high efficiency and high power density applications.

The authors of [9]-[13] studied the application of EPC enhanced mode GaN devices to MHz Buck converters and LLC resonant converters. They also discussed the impact of GaN device layout, magnetic components and distribution parameters on circuits. [13] shows the 3-D Integrated Gallium-Nitride-Based Point of Load Module Design in detail.

References [14], [15] presented a 90 W AC/DC adapter, which is composed of a buck-PFC stage and a Quasi-Switched-Capacitor (QSC) resonant DC/DC converter. The Buck-PFC evaluation module from TI Inc. achieves 97.1% peak efficiency with a GaN HEMT (TPH3006PD) and a SiC Schottky diode (C4D20120A) at 100 kHz. The 85 V/19 V. 1 MHz QSC resonant converter uses 100 V EPC eGaN FETs. In this case a 10.5 W/cm3 power density and 92.8% peak

Manuscript received Apr. 9, 2015; accepted Jul. 31, 2015
Recommended for publication by Associate Editor Joung-Hu Park.
†Corresponding Author: liyan@bjtu.edu.cn
Tel: +86-010-51687064-21, Beijing Jiaotong University
*School of Electrical Engineering, Beijing Jiaotong University, China
**Beijing Corona Science & Technology Co.,Ltd, Beijing, China

efficiency at 900 kHz are obtained.

This paper compares both the electrical properties of GaN FETs based on EPC and Si MOSFET, and the electrical characteristics of GaN Schottky diodes and Si fast recovery epitaxial diodes with the same voltage level. An evaluation of a GaN FET based on a flyback-forward high gain DC/DC converter at the soft-switching condition is presented in detail. A power loss analysis of the GaN FET based flyback-forward high gain DC/DC converter is discussed in detail. Finally, a 200W GaN FET based flyback-forward high gain DC/DC converter is established.

II. Structure and Characteristics of the GaN FET

A. Structure and Characteristics of the GaN FET

Fig. 1 shows the structure of a GaN FET. Si material is used as the substrate in the GaN FET, and a GaN crystal layer with a high resistance is grown on the basis of the Si substrate. An aluminum nitride (AlN) insulating layer is added between the GaN layer and the Si substrate layer isolating the device and the substrate. An AlGaN layer exists between the GaN layer and the gate (G), the source (S) and the drain (D) electrodes, and two-dimensional electron gas (2DEG) with high electron mobility and low resistance can be generated between the AlGaN layer and the GaN layer.

The device is voltage-controlled. When the positive gate-source voltage is greater than the threshold voltage, the gate is enabled, and with the 2DEG formed the transistor is turned on. When this is not the case, the transistor is turned off.

A GaN FET is a lateral structure device, as shown in Fig. 1. Unlike a Si MOSFET, a GaN FET has no parasitic body diode. There is no P-type parasitic bipolar region connected to the source electrode under the gate electrode of a GaN FET. This structure makes the GaN FET have a symmetrical transfer characteristic. As a result, the GaN FET can be driven either by a positive gate-to-source voltage (V_{gs}) or a positive gate-to-drain voltage (V_{gd}).

The GaN FET from EPC Inc. is an enhancement mode transistor, whose output characteristics with different gate-source voltages are shown in Fig. 2. For power conversion applications, this characteristic increases safety because the device is off when the driving voltage is below its threshold voltage. This decreases the designing difficulties in power conversion systems.

B. Characteristics of the GaN Schottky Diode

Compared with Si diodes, the GaN Schottky diode has a lower forward voltage, as shown in Fig. 3. The GaN Schottky diode exhibits a positive temperature coefficient because the forward voltage increases with an increase in temperature, while the Si diode shows a negative temperature coefficient.

The GaN Schottky diode also has lower on-state losses. In addition, the GaN Schottky diode has no minority carriers, which will greatly reduce transient voltage spikes.

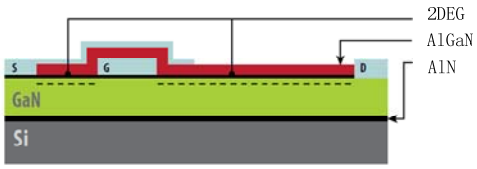

Fig. 1. Structure of GaN FET.

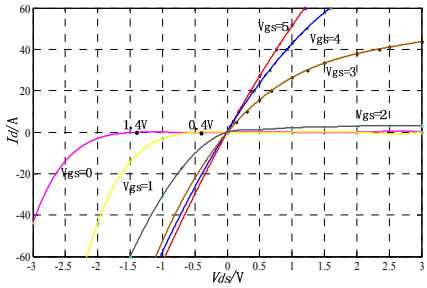

Fig. 2. Electrical characteristics of GaN FET.

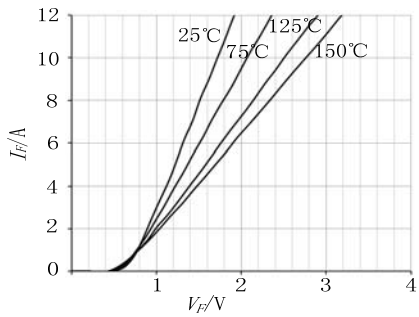

Fig. 3. Forward characteristics of GaN Schottky diode (TPS3410PK 600V/6A).

Furthermore, the GaN Schottky diode has a zero recovery charge. Si diodes, taking a Si fast recovery epitaxial diode DSEI12-06A as an example, typically have a 35ns recovery time and their recovery charge is typically 0.5uC under the condition of V_R=50V, $-di_F/dt$=200A/us, and I_F=14A, T=100°C.

III. Topology Analysis and Simulation Results of Flyback-Forward High Gain DC/DC Converters

A. Operation Principe and Soft-switching Behavior of Flyback-forward DC/DC Converters

A flyback-forward high gain DC/DC converter is shown in Fig. 4 [16]-[18]. The main switches S_1 and S_2 work in the interleaved mode, and their control signals have a 180 degree phase shift. The active-clamp circuits are mainly composed of auxiliary switches S_{c1} and S_{c2} and clamp capacitors C_{c1} and C_{c2}. The clamp switches S_{c1} and S_{c2} are driven complementarily by the main switches S_1 and S_2, which can recycle the leakage energy, suppress the turn-off voltage spikes on the main switches, and realize ZVS for all of the primary devices. In addition, there are two coupled inductors

in the converter L_1 and L_2, where the primary inductors L_{1a} and L_{2a} are coupled with the secondary inductors L_{1b} and L_{2b} respectively. L_{lk} is the total leakage inductance, which is equivalent to the secondary side. The key waveforms and equivalent circuits in different operational stages are shown in Fig. 5 and 6, respectively. The operation process description is given in detail as follows.

[t_0-t_1]: During this time, the main switches S_1 and S_2 are on and the two coupled inductors are charged by the input voltage in the flyback mode for energy storage. The auxiliary switches S_{c1} and S_{c2} are off. The output diodes D_{o1} and D_{o1} are both reverse-biased, and the output capacitors C_{o1} and C_{o2} provide energy to the load.

[t_1-t_2]: At t_1, the main switch S_2 is turned off. Its parasitic capacitor C_{s2} is charged so that the drain–source voltage of S_2 V_{ds2} increases. Since the GaN FET has a very small C_{ds}, the value of V_{ds2} increases quickly.

[t_2-t_3]: At t_2, V_{ds2} increases and the voltage on the primary inductor L_{2a} decreases resulting in a corresponding decrease in the voltage on the secondary inductor L_{2b} which makes the output diode D_{o1} conduct. During this time, the coupled inductor L_1 operates in the forward mode and L_2 works in the flyback mode to transfer energy to the load.

[t_3-t_4]: At t_3, the voltage on the parasitic capacitor C_{s2} increases to that on the clamp capacitor C_{c2} which makes the equivalent antiparallel diode of the clamp switch S_{c2} conduct. The coupled inductors L_1 and L_2 remain in the same mode as [t_2-t_3].

[t_4-t_5]: At t_4, the clamp switch S_{c2} is turned on with ZVS. The current through the equivalent antiparallel diode of the clamp switch S_{c2} transfers to S_{c2} quickly.

[t_5-t_6]: At t_5, the clamp switch S_{c2} is turned on. Due to the parasitic capacitor C_{s2}, V_{ds2} decreases linearly and that of the clamp switch S_{c2} increases in an approximately linear way. As a result, S_{c2} turns off with ZVS. One part of the leakage energy continues to be delivered to the load and another part of the leakage energy is recycled to the input source.

[t_6-t_7]: At t_6, V_{ds2} decreases to zero. Therefore, its equivalent antiparallel diode starts to conduct. The leakage current falls due to the voltage on the capacitor C_{o1}.

[t_7-t_8]: At t_7, the main switch S_2 turns on with ZVS. The secondary diode D_{o1} still conducts. At t_8, the leakage current decreases to zero and the diode D_{o1} turns off with the zero-current switching operation. The two primary inductors are again charged linearly by the input voltage.

B. Simulation of the flyback-forward DC/DC Converter

PSIM software is utilized to verify the operation principle of the circuit. The simulation parameters are listed as follows: V_{in}=25V, f_s=100kHz, V_o=380V, and the resistive load R_o=722Ω.

Waveforms of the primary side current I_{L1a}, I_{L2a} of the coupled inductor, the secondary diode current I_{Do1}, I_{Do2} and the driving signal V_{gs1}, V_{gs2} are shown in Fig. 7(a). A

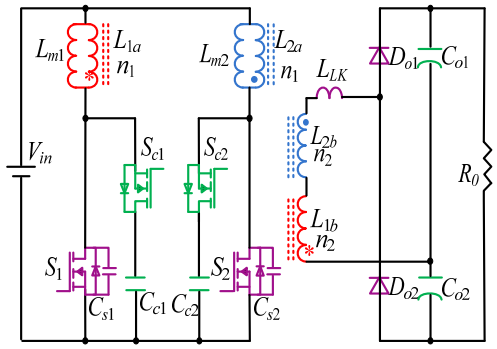

Fig. 4. Topology of flyback-forward high gain DC/DC converter.

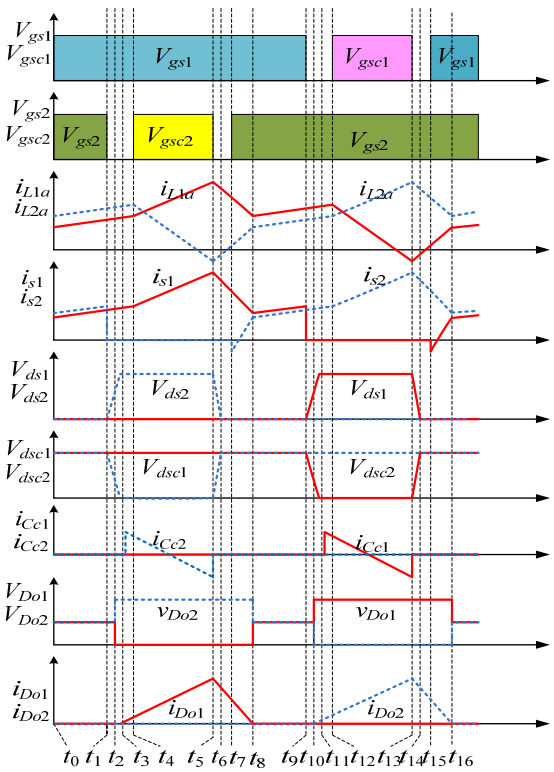

Fig. 5. Waveforms of flyback-forward high gain DC/DC converter.

waveform of the drain-source voltage V_{ds} of the main switches S_1, S_2 is shown in Fig. 7(b). The voltage and current of S_1 both without an active-clamp circuit and with an active-clamp circuit are shown in Fig. 7(c) and Fig. 7(d) respectively. Compared with the simulation results, without an active-clamp, the circuit with an active-clamp achieves ZVS turn on and ZCS turn off, which eliminates the voltage spikes of S_1 and S_2.

IV. Device Selection and Loss Analysis of the GaN FET Based Flyback-Forward High Gain DC/DC Converter

The design specifications of the GaN FET based flyback-forward high gain DC/DC converter are shown in Table I.

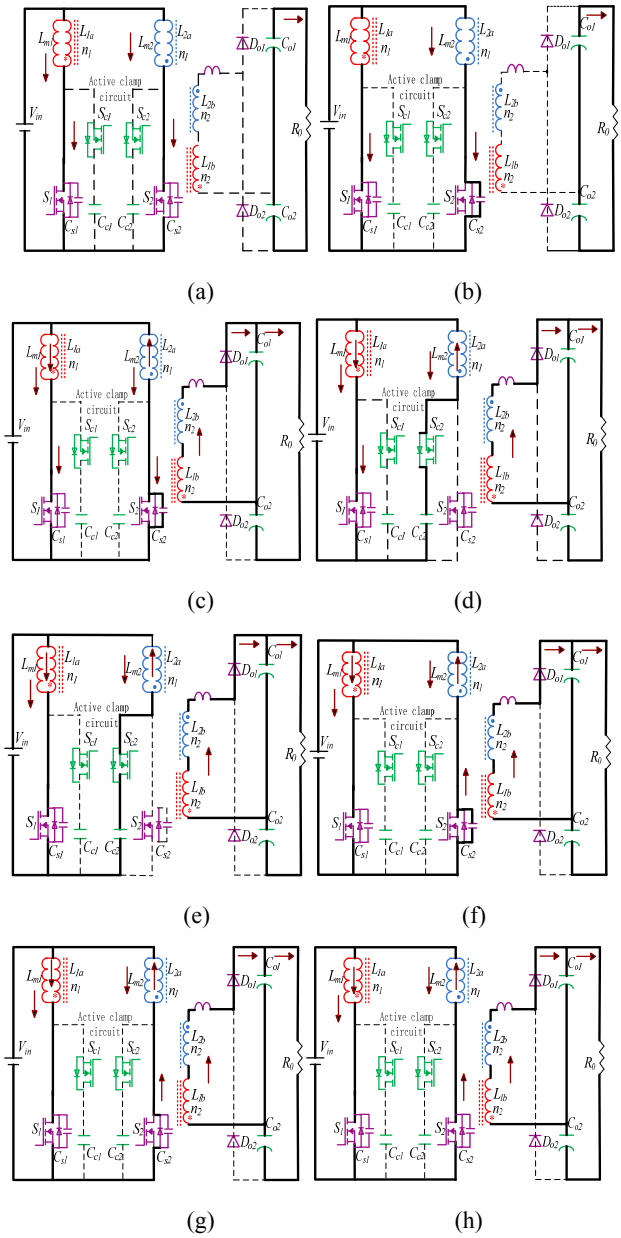

Fig. 6. Equivalent circuits of flyback-forward DC/DC circuit operational time intervals: (a) [t_0-t_1], (b) [t_1-t_2], (c) [t_2-t_3], (d) [t_3-t_4], (e) [t_4-t_5], (f) [t_5-t_6], (g) [t_6-t_7], and (h) [t_7-t_8].

A. Device and Component Selection of the Flyback-forward High gain DC/DC Converter

The main switch is selected by the voltage levels and current levels [19]. The voltage gain is:

$$\frac{V_{out}}{V_{in}} = \frac{2N}{1-D} \tag{1}$$

For a duty ratio of D>0.5, when V_{in} =40V, $N < 2.375$. In this case N=2. The main switch voltage is:

$$V_{ds\_S} = V_{ds\_Sc} = V_{in} + \frac{V_{out}}{N} = \approx 140V \tag{2}$$

The main switch current amplitude is:

TABLE I
DESIGN SPECIFICATION OF FLYBACK-FORWARD HIGH GAIN DC/DC CONVERTER

Input voltage	18-40V
Output voltage	380V
Power	200W
Switch frequency	100kHz

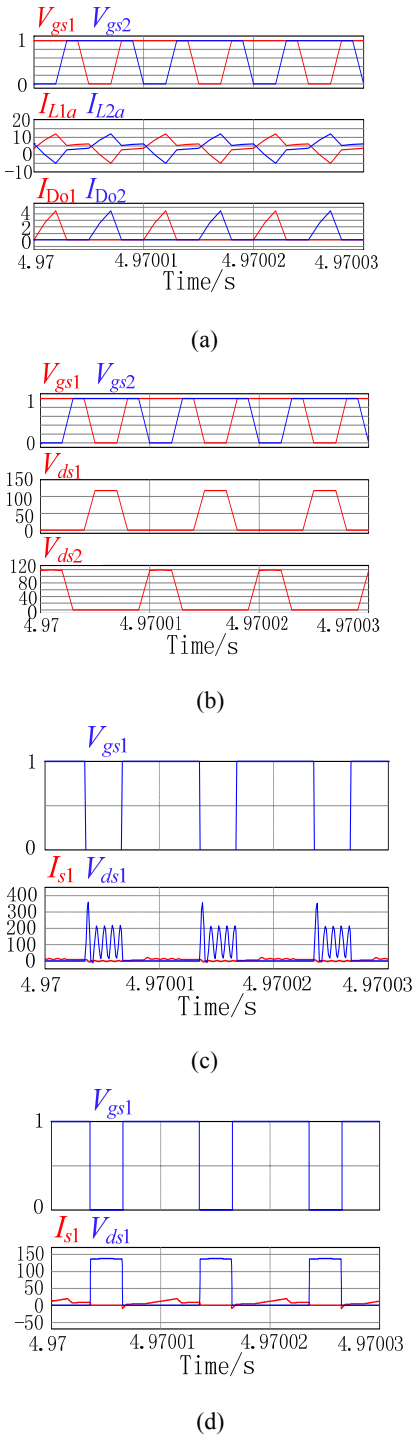

Fig. 7. Simulation waveforms of flyback-forward high gain DC/DC converter: (a) I_{L1a}, I_{L2a}, I_{Do1}, I_{Do2}, (b) V_{ds} of $S_1$and S_2, (c) results without active-clamp, and (d) results with active-clamp.

$$I_{S1} = \frac{P}{V_{in.\min}} = \frac{100}{18} \approx 5.6A \quad (3)$$

Therefore, two EPC2010 in parallel are employed as the main switches. Both the main and clamp switches have the same voltage stress. Therefore, the parameters of the clamp switches should be the same as the main switches. EPC2010s are selected as the clamp switches.

When the primary-side switch is turned off, the maximum voltage drop of the rectified diodes is about 350V. The peak current of the diodes is:

$$I_{Do\_peak} = ((N \cdot V_{Cc1} - V_{dc}/2) \cdot (1-D)/f_S)/L_{lk} \quad (4)$$

GaN Schottky diodes TPS3410PK 600V/6A produced by Transphorm Inc. are chosen as rectified diodes. The key parameters are shown in detail as following: V_F=1.3V, I_R= 25uA, Q_c=54nC, and C =81pF.

When coupled inductor turns ratio is N=2, the leakage inductance needs to satisfy the following condition:

$$L_{Lk} \le \frac{2 \cdot R_0 \cdot N^2 - M \cdot N \cdot R_0 \cdot (1-D)}{2 \cdot M^2 \cdot f_s} \quad (5)$$

The magnetizing inductor Lm can be determined by setting an acceptable current ripple, which is given by:

$$L_m = \frac{V_{in} \cdot D}{0.2 \cdot I_{Lm} \cdot f_S} \quad (6)$$

The magnetizing inductor is chosen as $L_m = 43.75\mu H$, $f_s = 100kHz$, and the leakage inductance of the primary side is L_{Lk_P}=0.87μH.

The two coupled inductors are composed of a planar EE core EE32 with 3F3 material and printed circuit boards as windings. The main parameters of the two coupled inductors are the same, and are shown in Table Π.

B. Loss Analysis of the flyback-forward High Gain DC/DC Converter

According to the symmetry of the circuit, switch S_1 is taken as an example to make a loss analysis. P_o=200W, V_{in}=25V, the conducting time of the main switch $T_1 = D*T_S$, the clamp switches conducting time is $T_2 = (1-D)*T_S$, and the dead time is 1% of the switching period *Ts*.

The active-clamp circuit leads to ZVS of S_1, whose loss is mainly composed of conduction loss and switching loss. According to Fig. 5, during one switching period, the current of S_1 in every stage is:

[t_0-t_3]: The current in one, which follows the primary of the coupled inductor, is defined by:

$$i_{L1a}(t) = I_{Lm1} = \frac{P_o}{2*V_{in}} \quad (7)$$

[t_3-t_5]: Because of the effect of the active clamp circuit, the leakage current of the secondary I_{Lk} increases linearly. Converting this to the primary, the main switch current is:

TABLE Π
DESIGN SPECIFICATION OF A COUPLED INDUCTOR

Copper thickness	0.3mm
Thickness of single board	0.9mm
Winding width	3mm
Clearance between layers	0.2mm
Number of primary layers	2
Number of primary turns	8
Number of secondary layers	4
Number of secondary turns	16

$$i_{L1a}(t) = I_{Lm1} + Ni_{Lk}(t) = I_{Lm1} + N\frac{(NV_{C_{c2}} - V_o/2)}{L_{Lk}}(t-t_3) \quad (t_3 < t < t_5) \quad (8)$$

where: $\Delta V = NV_{C_{c2}} - V_o/2 = 2V$, L_{Lk}=5μH.

[t_5-t_8]:

$$i_{L1a}(t) = I_{L1a}(t_5) - Ni_{Lk}(t) = I_{L1a}(t_5) - N\frac{V_o}{2L_{Lk}}t \quad (t_5 < t < t_8) \quad (9)$$

where: $t_5 - t_8 = \frac{(2*NV_{C_{c2}} - V_o)}{V_o} * T_2$.

[t_8-t_9]: During this stage, the main switches S_1 and S_2 are in the turn-on state. The current flowing through S_1 is that of the coupled inductor. According to the above analyses, the RMS current of S_1 is given by:

$$I^2_{L1a\_RMS} = \frac{1}{T_s}\int_0^{T_s} {i_{L1a}}^2(t)dt \quad (10)$$

When the R_{DS} of EPC2010 is 18mΩ, the conduction loss of S_1 is:

$$P_{S_1\_on} = {I_{L1a\_RMS}}^2 * R_{DS}/2 \quad (11)$$

The turn-off loss is:

$$P_{S_1\_of} = t_f f_s V_{peak\_S_1} I_{peak\_S_1}/6 \quad (12)$$

where t_f is the overlap time of I_{DS} and V_{DS}, and V_{peak_S1} is the peak voltage of the drain-source voltage.

Since the clamp switch is turned on under ZVS, the current flowing through the clamp switch can be expressed as:

$$i_{S_{c1}}(t) = I_{Lm1} - Ni_{Lk}(t) = I_{Lm1} - N\frac{(NV_{C_{c2}} - V_o/2)}{L_{Lk}}(t-t_3) \quad (t_{11} < t < t_{13}) \quad (13)$$

The RMS current of S_{c1} is:

$$I^2_{S_{c1}\_RMS} = \frac{1}{T_s}\int_0^{T_s} {i_{S_{c1}}}^2(t)dt \quad (14)$$

The active clamp switches are the same type as the main switches. Therefore, the conduction loss of S_{c1} is:

$$P_{S_{c1}\_on} = I^2_{S_{c1}\_RMS} * R_{DS} \quad (15)$$

Turn-off loss of S_{c1} is:

$$P_{S_{c1}\_sw} = t_f f_s V_{peak\_S_{c1}} I_{peak\_S_{c1}}/6 \quad (16)$$

The current of the secondary side diode is in the discontinuous current mode. As a result, the loss is mainly conduction loss.

[t_3-t_5]: The current increases linearly.

$$i_{D_{o1}}(t)=\frac{NV_{C_{c2}}-V_o/2}{L_{Lk}}(t-t_3)\ (t_3<t<t_5) \quad (17)$$

[t_5-t_8]: The secondary-side current decreases linearly.

$$i_{D_{o1}}(t)=I_{D_{o1}\_peak}-\frac{V_o/2}{L_{Lk}}(t-t_5) \quad (18)$$

The average current of D_{o1} is:

$$I_{D_{o1}\_avg}=\frac{1}{T_s}\int_0^{T_s} i_{D_{o1}}(t)dt \quad (19)$$

Conduction loss is:

$$P_{D_{o1}\_on}=I_{D_{o1}\_avg}V_F \quad (20)$$

where V_F is the forward voltage drop of the GaN Schottky diode, which is 1.3V.

The copper loss of a coupled inductor is estimated as follows.

$$P_{Cu\_p}=I_{rms\_p}^2R_{eq}=I_{rms\_p}^2*N_p*l_p*\frac{\rho}{A_{sp}} \quad (21)$$

where I_{rms_p} is the root mean square value of the primary current; N_p is the primary turns; l_p is the mean path length of the primary coil; ρ is the resistivity of copper at 100℃, which is $2.266*10^{-6}$ Ω*cm; and A_{sp} is the sectional area of the primary conductor.

The same method is used to estimate the copper loss of secondary side.

Then, the core loss is P_{Fe}, which is given by:

$$P_{Fe}=P_V*V_e \quad (22)$$

where P_V is about 0.4W/cm^3 for f_s=100kHz, B_{pk}=0.2T, and V_e=5.38cm^3.

The losses of the GaN FET based flyback-forward high gain DC/DC converter are shown in Table III. The total circuit loss is about 4.5W and the theoretical efficiency can reach 97.8%.

The losses of the Si MOSFET based flyback-forward high gain DC/DC converter are shown in Table IV. The total circuit loss is about 8.64W and theoretical efficiency can reach 95.86%.

TABLE III

POWER LOSS OF GAN FET BASED FLYBACK-FORWARD HIGH GAIN DC/DC CONVERTER

Conduction loss of S_1	0.18W
Turn off loss of S_1	0.47W
Conduction loss of S_{c1}	0.03W
Turn off loss of S_{c1}	0.23W
Conduction loss of D_{o1}	0.24W
Loss of a coupled inductor	2.35W
Driving loss	1W

TABLE IV

POWER LOSS OF SI MOSFET BASED FLYBACK-FORWARD HIGH GAIN DC/DC CONVERTER

Conduction loss of S_1	0.2W
Turn off loss of S_1	2.2 W
Conduction loss of S_{c1}	0.04W
Turn off loss of S_{c1}	0.9W
Conduction loss of D_{o1}	0.24W
Loss of a coupled inductor	3.5W
Driving loss	1.56W

V. EXPERIMENTAL RESULTS OF THE GAN FET BASED FLYBACK-FORWARD HIGH GAIN DC/DC CONVERTER

A. Experimental Comparison between the GaN FET and Si MOSFET Based on the flyback-Forward High Gain DC/DC Converter

When an EPC2010 is applied into a flyback-forward high gain DC/DC converter, the prototype is shown in Fig. 8. The unique Land Grid Array (LGA) package of EPC2010 products, the parasitic parameters in the main power circuit, and the driver circuit can be significantly reduced. This imporves the driving stability, while reducing the voltage stress of the main switches.

Experimental tests are conducted under the condition that the input voltage is 25V, the output power is 200W, the duty cycle of main switches is 0.74, and a GaN Schottky diode TPS3410PK is applied. The obtained experimental waveforms are shown in Fig. 9(a), where channel 1 is the output voltage (100V/div), channel 3 is V_{ds} of the main switches S_1 (50V/div), and channel 4 is the primary current of the coupled inductors I_{L1a} (5A/div). The temperatures of the devices are tested at a 30°C room temperature, as shown in the Fig. 9(b), where the hotter part is around main switches EPC2010s.

Fig. 10 shows the experimental results when the main switch is selected as a Si MOSFET IPB107N20N3G 200V/88A under the same operating conditions. Experimental tests are conducted under the condition that the input voltage is 25V and the output voltage is 380V. Only the main switches and the driver are changed.

In Fig. 10(a), channels 1 and 2 are V_{ds} of the main switches S_1 and S_2 (50V/div), channel 4 is the primary current of the coupled inductors I_{L1a} (10A/div), and channel 3 is the output voltage (100V/div). The temperatures of the devices were tested at a 30°C room temperature, as shown in the Fig. 10(b), where the hotter part is around main switches IPB107N20N3G.

From the Fig. 9(a), it can be concluded that there is no voltage spikes when the main switch S_1 is turned off, and that switching loss of the GaN FET is small. The output DC voltage of the circuit can be stabilized at 380V. On the other hand, there is a visible voltage spikes of the Si MOSFET

Fig. 8. PCB board of GaN FET based flyback-forward high gain DC/DC Converter.

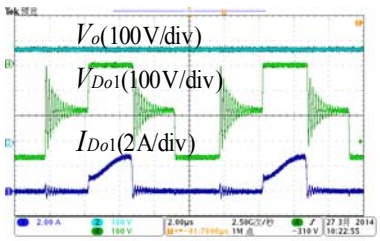

(a)

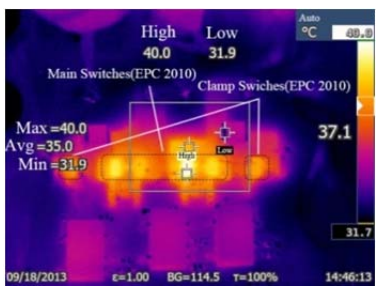

(b)

Fig. 9. Test results of GaN FET based flyback-forward high gain DC/DC converter (a) experimental waveforms, (b) thermal test results.

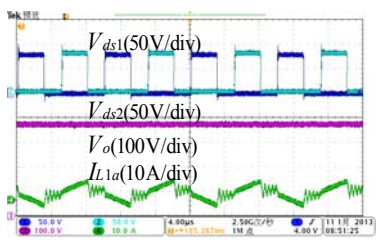

(a)

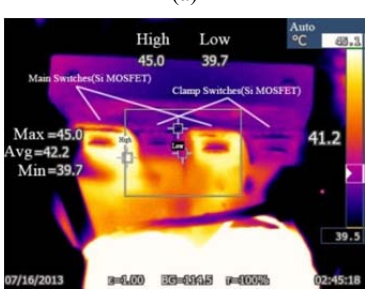

(b)

Fig. 10. Test results of Si MOSFET flyback-forward high gain DC/DC converter: (a) experimental waveforms and (b) thermal test results.

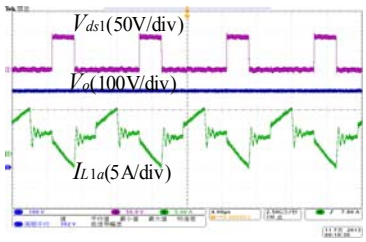

(a)

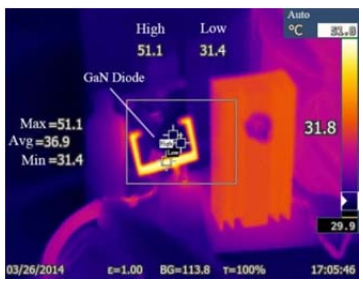

(b)

Fig. 11. Test results of GaN FET based flyback-forward high gain DC/DC converter applying GaN diodes: (a) experimental waveforms and (b) thermal test results of TPS3410PK.

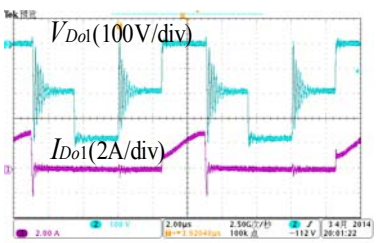

(a)

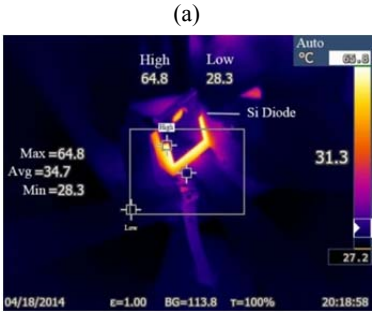

(b)

Fig. 12. Test results of GaN FET based flyback-forward high gain DC/DC converter applying Si diodes: (a) experimental waveforms and (b) thermal test results of DSEI12-06A.

based flyback-forward high gain DC/DC Converter, which results in a decreased efficiency. The temperature of the Si MOSFET is higher than that of the GaN FET under the same operating conditions.

The highest efficiency is 95.8% at the 200W power point of the GaN FET based flyback-forward high gain DC/DC converter. Meanwhile, it is only 94% at the 200W power point of the Si MOSFET based converter. From the experimental results, it can be seen that the application of the

GaN device can reduce the voltage stress of the switches and increase the circuit efficiency.

B. Experimental Comparison between the GaN Diode and the Si Diode Based on a Flyback-Forward High Gain DC/DC Converter

Based on a flyback-forward high gain DC-DC converter applying a EPC2010, an experimental comparison between the GaN diode and the Si diode with the same 600V voltage level is made to determine the advantages of the GaN diode.

Experimental tests are conducted under the condition that the input voltage is 25V, the output power is 200W, the duty cycle of the main switches is 0.74, and GaN Schottky diodes TPS3410PK are applied. The obtained experimental waveforms are shown in Fig. 11(a), where channel 1 is the current of D_{o1} I_{Do1}(2A/div), and channel 4 is the forward voltage of D_{o1} V_{Do1}(100V/div). Fig. 11(b) shows the temperature test results of the TPS3410PK at a 30°C room temperature, where highest temperature is 51.1°C.

Under the same conditions, Si fast recovery epitaxial diodes DSEI12-06A manufactured by IXYS are applied to the converter for comparative purposes. The results are shown in Fig. 12(a), where channel 2 is the forward voltage of D_{o1} V_{Do1}(100V/div), and channel 3 is the current of D_{o1} I_{Do1}(2A/div). Fig. 12(b) shows temperature test results of the DSEI12-06A at a 30°C room temperature, where highest temperature is 64.8°C.

From Fig. 11(a), it can be concluded that there is little reverse recovery current when the diode is turned off and it verifies the zero recovery charge. Meanwhile from Fig. 12(a), a larger reverse recovery current appears compared with Fig. 11(a). In addition, the voltage spike is larger than that shown in Fig. 11(a) during reverse recovery time, which reduces efficiency. Comparing Fig. 11(b) and Fig. 12(b), it can be seen that the Si diode has a higher temperature under the same operating conditions as the GaN diode. This indicates a larger loss.

VI. CONCLUSION

This paper describes the development of a GaN FET and presents its structure and electrical properties. A GaN FET manufactured by EPC Inc. is applied in a flyback-forward high gain DC/DC converter. A loss analysis is discussed in detail for the GaN FET based flyback-forward high gain DC-DC converter. The application of the GaN FET can significantly reduce the switch off voltage spike, and reduce switching losses. An experimental comparison between a GaN diode and a Si diode is made to determine the advantages of the GaN diode. Finally, a 200W GaN FET based flyback-forward high gain DC/DC converter is established. Experimental results verify that the GaN FET is superior to the Si MOSFET, and that the GaN Schottky diode is superior to the Si fast recovery epitaxial diode at the same voltage level.

REFERENCES

[1] A. Lidow, J. Strydom, M. Rooij, and Y. Ma, *GaN transistors for efficient power conversion*, Power Conversion Publications, 2nd, 2012.

[2] K. S. Boutros, R. Chu, and B. Hughes, "Gan power electronics for automotive application," *Energytech*, pp.1-4, 2012.

[3] T. Morita, S. Tamura, Y. Anda, M. Ishida, Y. Uemoto, T. Ueda, T. Tanaka, and D. Ueda. "99.3gan-based gate injection transistors," *Applied Power Electronics Conference and Exposition (APEC)*, pp.481-484, 2011.

[4] S. Tamura, Y. Anda, M. Ishida, Y. Uemoto, T. Ueda, T. Tanaka, and D. Ueda, "Recent advances in gan power switching devices," *Compound Semiconductor Integrated Circuit Symposium(CSICS)*, pp.1-4, Oct. 2010.

[5] M. J. Scott, J. Li, and J. Wang, "Applications of Gallium Nitride in power electronics," *Power and Energy Conference at Illinois(PECI)*, pp. 1-7, Feb. 2013.

[6] M. J. Scott, K. Zou, E. Inoa, R. Duarte, Y. Huang, and J. Wang, "A Gallium Nitride switched-capacitor power inverter for photovoltaic applications," *Applied Power Electronics Conference and Exposition(APEC)*, pp.46-52, Feb. 2012.

[7] M. J. Scott, K. Zou, J. Wang, C. Chen, M. Su, and L. Chen, "A Gallium Nitride Switched-Capacitor Circuit Using Synchronous Rectification," *IEEE Trans. Ind. Appl*., Vol. 49, No. 3, pp.1383-1391, May/Jun. 2013.

[8] J. Delaine, P. O. Jeannin, D. Frey, and K. Guepratte, "Improvement of GaN transistors working conditions to increase efficiency of A 100W DC-DC converter," *Applied Power Electronics Conference and Exposition(APEC)*, pp. 656-663, Mar. 2013.

[9] X. Ren, D. Reusch, S. Ji, Z. Zhang, M. Mu, and F. C. Lee, "Three-level driving method for GaN power transistor in synchronous buck converter," *Energy Conversion Congress and Exposition(ECCE)*, pp.2949-2953, Sep. 2012.

[10] D. Reusch , F. C. Lee , D. Gilham , and Y. Su, "Optimization of a high density gallium nitride based non-isolated point of load module," *Energy Conversion Congress and Exposition(ECCE)*, pp.2914-2920, Sep. 2012.

[11] S. Ji, D. Reusch, and F. C. Lee, "High-Frequency High Power Density 3-D Integrated Gallium-Nitride-Based Point of Load Module Design," *IEEE Trans. Power Electron.*, Vol. 28, No. 9, pp. 4216-4226, Sep. 2013.

[12] F. C. Lee and Q. Li, "High-Frequency Integrated Point-of-Load Converters: Overview," *IEEE Trans. Power Electron.*, Vol. 28, No. 9, pp. 4127-4136, Sep. 2013.

[13] S. Ji, D. Reusch, and F. C. Lee, "High-Frequency High Power Density 3-D Integrated Gallium-Nitride-Based Point of Load Module Design," *IEEE Trans. Power Electron.*, Vol. 28, No. 9, pp. 4216-4226, Sep. 2013.

[14] X. Zhang, C. Yao, M. J. Scott, E. Davidson, J. Li, P. Xu, and J. Wang, "A GaN Transistor based 90 W Isolated Quasi-Switched-Capacitor DC/DC Converter for AC/DC Adapters," *IEEE Workshop on Wide Bandgap Power Devices and Applications(WiPDA)*, pp. 15-12, Oct. 2013.

[15] X. Zhang, C. Yao., X. Lu, E. Davidson, M. Sievers, M. J. Scott, P. Xu, and J. Wang, "A GaN Transistor based 90W AC/DC Adapter with a Buck-PFC Stage and an Isolated Quasi-Switched-Capacitor DC/DC Stage," *Applied Power Electronics Conference and Exposition(APEC)*, pp. 109-116, Mar. 2014.

[16] J. H. Lee, J. H. Park, and H. Jeon, "Series-connected forward-flyback converter for high step-up power

conversion," *IEEE Trans. Power Electron*., Vol. 26, No. 12, pp. 3629-3641, Dec. 2011.
[17] W. Li, P. Li, H. Yang, and X. He, "Three-level forward–flyback phase-shift zvs converter with integrated series-connected coupled inductors," *IEEE Trans. Power Electron*., Vol. 27, No. 6, pp. 2846-2856, Jun. 2012.
[18] D.-H. Kim, J.-H. Jang, J.-H. Park, and J.-W. Kim, "Single-ended high-efficiency step-up converter using the isolated switched-capacitor cell," *Journal of Power Electronics*, Vol. 13, No. 5, pp.766-778, 2013.
[19] J.-M. Kwon, E.-H. Kim, B.-H. Kwon, K.-H. Nam, "High-efficiency fuel cell power conditioning system with input current ripple reduction," *IEEE Trans. Ind. Electron.*, Vol. 56, No. 3, pp. 826-834, Mar. 2009.

Yan Li was born in Heilongjiang Province, China, in 1977. She received her B.S. and M.S. degrees in Electrical Engineering from Yanshan University, Qinhuangdao, China, in 1999 and 2003, respectively; and her Ph.D. degree in Electrical Engineering from the Nanjing University of Aeronautics and Astronautics, Nanjing, China, in 2009. From 1999 to 2009, she was at Yanshan University. Since 2009, she has been in the School of Electrical Engineering, Beijing Jiaotong University, Beijing, China. Her current research interests include multiple-input dc/dc converters, renewable power systems, and PV grid-tied systems.

Trillion Q. Zheng (Qionglin Zheng) (M'06-SM'07) was born in Jiangshan, Zhejiang Province, China, in 1964. He received his B.S. degree in Electrical Engineering from Southwest Jiaotong University, Sichuan, China, in 1986; and his M.S. and Ph.D. degrees in Electrical Engineering from Beijing Jiaotong University, Beijing, China, in 1992 and 2002, respectively. He is presently a Distinguished Professor at Beijing Jiaotong University. He directs the Center for Electric Traction, founded by Ministry of Education, China. His current research interests include the power supplies and AC drives of railway traction systems, high performance and low loss power electronics systems, PV based converters and control, and active power filters and power quality correction. He holds 17 Chinese patents, and has published over 60 journal articles and more than 100 technical papers in conference proceedings. From 2003 to 2011, he served as the Dean of the School of Electrical Engineering, at Beijing Jiaotong University. He is presently the Deputy Director of the Beijing Society for Power Electronics and a Member of the China Electrotechnical Society. He received an Excellent Teacher Award of the Beijing Government (1997), and a Youth Award of Railway Science and Technology of Zhan Tianyou (2005). He is a laureate of the Youth Elite of Science and Technology of the Railway Ministry of China (1998) and a Zhongda Scholar for power electronics and motor drives of the Delta Environmental and Educational Foundation (2007).

Yajing Zhang was born in Hebei Province, China, in 1984. She received her B.S. and Ph.D. degrees in Electronic Engineering from Beijing Jiaotong University, Beijing, China, in 2008 and 2014, respectively. Her current research interests include PV grid-tied systems and wide band gap semiconductors.

Meiting Cui was born in Hebei Province, China, in 1990. She received her B.S. degree in Electrical Engineering from Yanshan University, Qinhuangdao, China, in 2011; and her M.S. degree in Electronic Engineering from Beijing Jiaotong University, Beijing, China, in 2014.

Yang Han was born in Harbin, China, in 1979. He received the B.S. degrees in electrical engineering from the Beijing Institute of Technology, beijing, China, in 2003.He focused on switch mode power supply research. Since from 2013, he have been working in Beijing Corona Science & Technology Co. Ltd, where he is currently a project manager. His research interests include micro inverter products development for renewable energy applications and switch mode power supply.

Wei Dou was born in Chengde, China, in 1977. He received the B.S. and M.S. degrees in electrical engineering from the Sichuan University, Chengdu, China, in 2000 and 2004, respectively, and the Ph.D. degree in power electronics and drives from IEE, CAS, Beijing, China, in 2008. Since 2008, he joined IEE, CAS, as an assistant researcher, and became associate researcher in 2010. In CAS, he focused on high power grid-connected inverter research. Since from 2011, he have been working in Beijing Corona Science & Technology Co., Ltd, where he is currently a chief engineer. His research interests include the advanced control strategy of high power inverter and power electronics products development for renewable energy applications.